ISSN (ONLINE): 2454-9762
ISSN (PRINT): 2454-9762
Available online at www.ijarmate.com

International Journal of Advanced Research in Management, Architecture, Technology and Engineering (IJARMATE)
Vol. 2, Issue 3, March 2016

Automated Diagnosis of Intracardiac Tumor for Echocardiogram

P.Kalaiselvi[1], N.Suganya[2], S.Vigneshwaran[3]

kalai8290@gmail.com[1],suganyaece50@gmail.com[2],vigneshwaran18371@gmail.com[3]

Assistant professor, ECE, N.S.N College of Engineering & Technology, karur, India. [1]

UG Scholar, ECE Department, N.S.N College of Engineering & Technology, karur, India [2]

UG Scholar, ECE Department, N.S.N College of Engineering & Technology, karur, India [3]

***Abstract*— This project present novel method is proposed to classify the intracardiac tumor and thrombi in echocardiograms. Different from other approaches, the contribution of this method is incorporating the sparse representation methodology into the whole algorithm. The proposed method may offer several useful innovations. Identification of intracardiac masses in echocardiograms is one important task in cardiac disease diagnosis. To improve diagnosis accuracy, a novel fully automatic classification method based on the sparse representation is proposed to distinguish intracardiac tumor and thrombi in echocardiography. A novel globally denoising approach combing the K-SVD and the NLM is employed to eliminate the speckle. The globally despeckling algorithm yields better noise attenuation and edge enhancement, without destroying the important cardiac structures. Ninety –seven clinical echocardiogram sequences are collected to assess the effectiveness. Compared with other state of the classifier, our proposed method demonstrates the best performance by achieving an accuracy of 96.91%, sensitivity of 100%, and as specificity of 93.02%. It explicates that our mind capable of classifying intracardiac tumors and thrombi in echocardiography.**

***Index Terms*— Intracardiac tumor and thrombi, K-SVD, NLM, denoising, despeckling algorithm..**

I. INTRODUCTION

Digital image processing is the use of computer algorithms to perform image processing on digital images. As a subcategory or field of digital signal processing, digital image processing has many advantages over analog image processing. It allows a much wider range of algorithms to be applied to the input data and can avoid problems such as the build-up of noise and signal distortion during processing. Since images are defined over two dimensions (perhaps more) digital image processing may be model in the form of multidimensional systems.

Cardiac tumors represent a relatively rare, yet challenging diagnosis. Secondary tumors are far more frequent than primary tumors of the heart. The majority of primary cardiac tumors is benign in origin, with primary malignant tumors accounting for 25% of cases. Metastatic tumors usually arise from lung, breast, renal cancer, Melanomas and lymphomas. Clinical manifestations of cardiac tumors depend on the size and location of the mass and the infiltration of adjacent tissues rather than the type of the tumor itself. Echocardiography is the main diagnostic tool for the detection of a cardiac mass. Other imagings modalities (C-MRI, C-CT, 3D Echo) may offer further diagnostic information and the establishment of the diagnosis is made with histological examination. Management depends on the type of the tumor and the symptomatology of the patient.

Metastatic cardiac tumors are far more frequent (approximately from 30- to 40-fold) than primary tumors of the heart. They usually arise from melanomas, lung, breast, and renal cancer, as well as lymphomas. Metastases may originate from blood dissemination of cancer cells, direct extension via adjacent tissues, or propagation via the superior or the inferior vena cava to the right atrium. Pericardium is most often affected, resulting in pericardial effusion which may contain masses comprising either cancer cells or blood clots and fibrin.

The imaging techniques that are used when there is a suspicion for the occurrence of a cardiac tumor, as well as for the differential diagnosis of other cardiac masses like vegetations and thrombi, are mainly echocardiography, magnetic resonance imaging (MRI), and computed tomography (CT) of the heart. Chest X-ray can offer indirect findings from the enlargement of cardiac chambers, the occurrence of calcification, or pericardial effusion.

II. K-SVD PHRASE REPRESENTATION

The K-SVD algorithm is quite computationally demanding, however, especially when the dimensions of the dictionary increase or the number of training signals becomes large. In this paper, efficient implementation of the algorithm which reduces its complexity as well as its memory requirements was discussed. The improvements are achieved by using a modified dictionary update step which replaces the explicit SVD computation with a simpler approximation, and employing an optimized OMP implementation which accelerates the sparse-coding step.

ISSN (ONLINE): 2454-9762
ISSN (PRINT): 2454-9762
Available online at www.ijarmate.com

International Journal of Advanced Research in Management, Architecture, Technology and Engineering (IJARMATE)
Vol. 2, Issue 3, March 2016

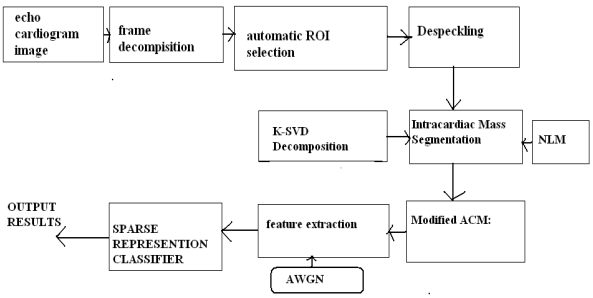

Fig. 1. Workflow diagram for the proposed classification method.

A. Frame Decomposition

The cardiologists acquire echocardiogram sequences when diagnosing the disease. To segment the intracardiac mass and evaluate its movement, the echocardiography sequences are divided into consecutive frames beforehand. The typical duration of an echocardiogram sequence is about 3–4 s. The frame rate is 39 frames per second. Each decomposed frame is 480 × 640 pixels. Besides the scanned region, an echocardiogram depicts texts and labels, containing information about the patient and scanning transducer, as shown in Fig. 1. Compared with moving heart in two successive frames, these texts and labels are static. After subtraction of two successive frames, the static information are all removed, while the sector scanned region containing moving heart is remained. Then, the profile of the sector scanned region is detected and a rectangle covering the sector is identified. Finally, the original image is cropped to keep the scanned region for further analysis.

B. Automatic ROI Selection

In order to focus on the mass area, a ROI containing the mass and its surrounding tissues are defined. A coarse-to-fine iteration strategy for sub windows clustering is applied to automatically select the ROI. Fig. 1 depicts that compared with the mass and the myocardium, the cardiac chamber owns unique texture features, with lower intensities and uniformed distributions. Such intensity differences help to assort the images into two classes: the uniform areas (chamber) and the texture areas (the mass or the myocardium).

C. Globally Despeckling by the K-SVD Decomposition and the NLM

For ultrasound images, the speckle is a Rayleigh-distributed multiplicative noise. It degrades the contrast resolution, limiting the delectability of small, low-contrast lesions. Different from locally based denoising methods, the NLM extends the "neighborhood" to the "whole image," taking advantage of the high degree of redundancy in an image. Usually for a fixed configuration, many similar samples can be found in the whole image. With the help of these related patches in far-away areas, rather than the irrelevant ones in local neighborhood, the denoising performance will be greatly improved, especially in the edge preservation.

D. Intracardiac Mass Segmentation

As the basis for the further features extraction, extracting the boundary of the mass is of great importance. Since the intracardiac mass has a base connected with the atrial wall, the mass and the atrial wall should be segmented together.

E. Feature Extraction

When identifying intracardiac mass in an echocardiogram sequence, usually the cardiologists make the judgment based on two rules: the motion feature (the mass movement) and the boundary feature (the base length). Although two masses show differences in echo reflections, texture characteristics are visually indistinguishable due to the poor image quality. They are always omitted clinically. However, texture features, especially the mass internal echo is quite important in the classification. Here, for each segmented mass, three types of features are computed: the motion feature, the boundary feature, and the
proposed texture features.

F. Sparse Representation-Based Classifier

A sparse representation-based classifier (SRC) is used to identify an intracardiac mass. It relies on the idea that the test sample can be represented as a linear combination of the training sample. Different from other classifiers, the SRC is a nonparametric learning method which does not need a training process but only need the training data.

III. Methods

The segmentation techniques usually consider the pixel along a boundary and pixel contained in the region. And an approach to obtain the descriptor that is compact the data into representation. There are several approaches above.

A. Chain Code

The chain code is used to represent a boundary by the length and the direction of straight-line segments. Typically, this representation is based on 4- or 8- connectivity of the segments.

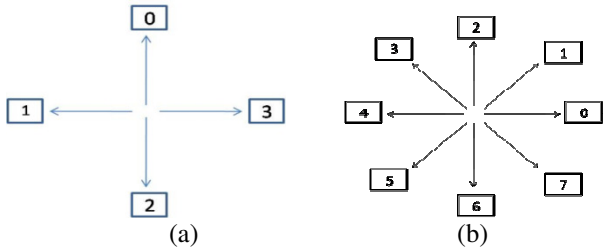

Fig.1. (a) 4-directional chain code (b) 8-directional chain code.

ISSN (ONLINE): 2454-9762
ISSN (PRINT): 2454-9762
Available online at www.ijarmate.com

International Journal of Advanced Research in Management, Architecture, Technology and Engineering (IJARMATE)
Vol. 2, Issue 3, March 2016

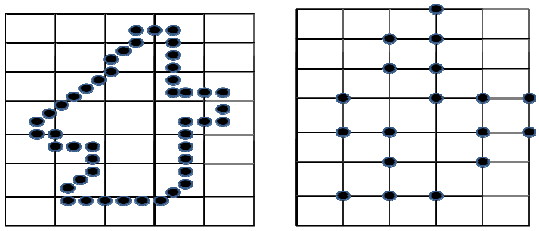

(a) (b)

Digital images are usually processed in a grid format, but it may not match shape of the boundary if the chain of codes is quite long or the boundary is distributed by the noise. An approach frequently used to circumvent the problems just discussed is to resample the boundary by selecting a larger grid spacing. It can be seen that the accuracy and samples is related to grid spacing.

B. *Polygonal Approximations*

The goal of polygonal approximation is to capture the essence of the boundary shape with the fewest possible polygonal segments. Several polygonal approximation techniques of middle complexity and processing requirements are suitable for image processing applications.

Minimum Perimeter Polygons

We visualize this enclosure as two walls corresponding to the outside and inside boundaries of the strip of cells, and think of the object boundary as a rubber band contained within the wall. If the rubber band is allowed to shrink, it takes the shape shown in Fig.2.

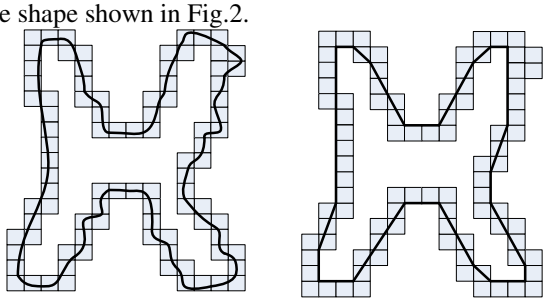

(a) (b)

Fig.2 (a) Object boundary enclosed by cells, and (b) Minimum perimeter polygon.

C. *Merging Techniques*

Merging techniques based on average error or other criteria have been applied to the problem of polygonal approximation. The approach is to merge points along a boundary until the least square error line fit of the points merged so far exceeds a preset threshold.

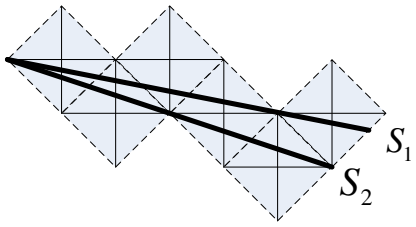

Fig.3. Merge approach of a set of digital boundary

D. *Splitting Techniques*

An approach of the splitting techniques is subdivided a segment successively into two part until a criterion is satisfied. For instance, a requirement might be that the maximum perpendicular distance from a boundary segment to the line joining its two end points not exceeds a preset threshold.

Signature is a approach that translate 2-D function to 1-D function. One of the simplest is to plot the distance from the center to the boundary as a function of angle, as illustrated in Fig.6.3.

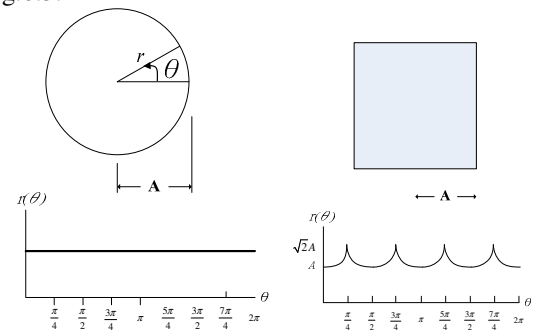

(a) (b)

Fig.1.18 (a), (b): Distance signature of circle and rectangular shapes.

Decomposing a boundary into segments often is useful. Decomposition reduces the boundary's complexity. This approach is useful when the boundary contains one or more concavities. In this case use of the convex hull of the region enclosed by the boundary is a powerful tool for robust decomposition of the boundary.

Skeletons mean thinning. The skeleton of a region may be defined via the MAT (medial axis transformation) proposed by Blum [1967]. According to the definition, the step 1 flags a contour point p_1 for deletion if the following conditions are satisfied:

$$\text{(a) } 2 \le N(p_1) \le 6$$

$$\text{(b) } T(p_1) = 1$$

$$\text{(c) } p_2 \square p_4 \square p_6 = 0$$

$$\text{(d) } p_4 \square p_6 \square p_8 = 0 \qquad (1)$$

Where $N(p_1)$ is the number of nonzero neighbors of p_1 : that is,

$$N(p_1) = p_2 + p_3 + \ldots\ldots + p_8 + p_9 \qquad (2)$$

p_9	p_2	p_3
p_8	p_1	p_4
p_7	p_6	p_5

Fig.6.5 Neighborhood arrangement used by the thinning algorithm

ISSN (ONLINE): 2454-9762
ISSN (PRINT): 2454-9762
Available online at www.ijarmate.com

International Journal of Advanced Research in Management, Architecture, Technology and Engineering (IJARMATE)
Vol. 2, Issue 3, March 2016

In section 2, conditions (a) and (b) remain the same, but conditions (c) and (d) are changed to

$$(c') \quad p_2 \square p_4 \square p_8 = 0$$
$$(d') \quad p_2 \square p_6 \square p_8 = 0 \qquad (3)$$

The iteration of the thinning algorithm consists of (1) applying step 1 to flag border points for deletion; (2) deleting the flagged points; (3) applying step 2 to flag the remaining border points for deletion; and (4) deleting the flagged points. In this section, we discuss boundary descriptors and regional descriptors.

E. Boundary Descriptors

There are several approaches to describe the boundary of a region. We illustrate as follows.There are several simple descrioptors. Just like basic rectangular, eccentricity, curvature and so on. Basic rectangular is the rectangular that generate by major axis and minor axis. Eccentricity is the ratio of major axis and minor axis. Curvature is defined as the rate of the boundary that use convex and concave to describe the boundary.

The first difference of a chain-coded boundary depends on the starting point. The shape number of such a boundary, based on the 4-directional code is defined as the first difference of smallest magnitude. For a desired shape order, we find the rectangle of order n whose eccentricity best approximates that of the basic rectangle and use this new rectangle to establish the grid size.

F. Fourier Descriptors

The Fourier descriptors are starting at an arbitrary point (x, y). Each coordinate pair can be treated as a complex number so that

$$s(k) = x(k) + jy(k) \qquad (4)$$

This representation has one great advantage that it reduces a 2-D to a 1-D problem. The discrete Fourier transform (DFT) of $s(k)$ is

$$a(u) = \frac{1}{K}\sum_{k=0}^{K-1} s(k)e^{-j2\pi uk/K} \qquad (5)$$

for $u = 0,1,2,.....,K-1$ .The complex coefficients $a(u)$ are called the Fourier descriptors of the boundary. The inverse Fourier transform of these coefficients restore $s(k)$. That is,

$$s(k) = \sum_{u=0}^{K-1} a(u)e^{j2\pi uk/K} \qquad (6)$$

for $k = 0,1,2,...., K-1$. Suppose, however, that instead of all the Fourier coefficients, only the first P coefficient is used. This is equivalent to setting $a(u) = 0$ for $u > P-1$. The result is the following approximation to $s(k)$:

$$\hat{s}(k) = \sum_{u=0}^{P-1} a(u)e^{j2\pi uk/K} \qquad (7)$$

The smaller P becomes, the more detail that is lost on the boundary. And the bigger P becomes, it more similar to boundary.

G. Statistical Moments

The shape of boundary segments can be described quantitatively by using simple statistical moments, such as the mean, variance, and higher-order moments. Let us treat the amplitude of g as a discrete random variable v and form an amplitude histogram $p(v_i), i = 0,1,2,....A-1$, where A is the number of discrete amplitude increments in which we divide the amplitude scale, and p() is the probability of value vi. The equation of nth moment about its mean is

$$u_n(v) = \sum_{i=0}^{A-1} (v_i - m)^n p(v_i) \qquad (8)$$

where

$$m = \sum_{i=0}^{A-1} v_i p(v_i) \qquad (9)$$

An alternative approach is to normalize g(r) to unit area and treat it as a histogram. In other words, $g(r_i)$ is now treated as the probability of value r_i occurring. In this case, r is treated as the random variable and the moments are

$$u_n(r) = \sum_{i=0}^{K-1} (r_i - m)^n g(r_i) \qquad (10)$$

where

$$m = \sum_{i=0}^{K-1} r_i g(r_i) \qquad (11)$$

In this notation, K is the number of points on the boundary, and $u_n(r)$ is directly related to the shape of $g(r)$. Basically, what we have accomplished is to reduce the description task to that of describing 1-D functions. The advantage of moments over other techniques is that implementation of moments is carry a physical explain of boundary shape and this approach is insensitive to rotation.

H. Statistical approaches

Statistical approaches yield characterizations of textures as smooth, coarse, and grainy, and so on. One of the approaches for describing texture is to use statistical moments of the gray-level histogram of an image or region. The nth moment of z about the mean is

$$u_n(z) = \sum_{i=0}^{L-1} (z_i - m)^n p(z_i) \qquad (12)$$

Where

$$m = \sum_{i=0}^{L-1} z_i p(z_i) \qquad (13)$$

The second moment is important. It is a measure of gray- level contrast that can be used to establish descriptors of relative smoothness. For example, the measure of constant intensity

$$R = 1 - \frac{1}{1+\sigma^2(z)} \qquad (14)$$

The third moment is a measure of the skewness of the histogram. The fourth moment is a measure of its relative

ISSN (ONLINE): 2454-9762
ISSN (PRINT): 2454-9762
Available online at www.ijarmate.com

International Journal of Advanced Research in Management, Architecture, Technology and Engineering (IJARMATE)
Vol. 2, Issue 3, March 2016

flatness. The fifth and higher moments are not so easily related to histogram shape. Some useful approaches established in the histogram is measuring of uniformity

$$U = \sum_{i=0}^{L-1} p^2(z_i) \quad (15)$$

and measuring of an average entropy

$$e = -\sum_{i=0}^{L-1} p(z_i)\log_2 p(z_i) \quad (16)$$

I. *Structural Approaches*

Structural techniques deal with the arrangement of image primitives. Suppose that we have a rule of the form $S \to aS$, which indicates that the symbol S may be rewritten as aS. If a represents a circle [Fig.3.2.3 (a)] and the meaning of "circles to the right" is assigned to a string of the form aaa…., the rule $S \to aS$ allows generation of the texture pattern.

J. *Spectral Approaches*

Spectral techniques are based on properties of the Fourier spectrum and are used primarily to detect global periodicity in an image by identifying high energy, narrow peaks in the spectrum. Interpretation of spectrum features just mentioned often are simplified by expressing the spectrum in polar coordinates to yield a function $S(r,\theta)$, where S is the spectrum function and r and θ are the variables in this coordinate system. Analyzing $S_\theta(r)$ for a fixed value of θ yield the behavior of the spectrum along a radial direction from the origin, whereas analyzing $S_r(\theta)$ for a fixed value of r yields the behavior along a circle centered on the origin.

$$S(r) = \sum_{\theta=0}^{\pi} S_\theta(r) \quad (17)$$

$$S(\theta) = \sum_{r=1}^{R_0} Sr(\theta) \quad (18)$$

The material discussed is applicable to boundaries and regions. Suppose that we are given the n component images of such a color. The n images can be treated as a unit by expressing each group of n corresponding pixels as a vector. These n elements con be expressed in the form of a 3-D column vector, x where

$$x = \begin{bmatrix} x_1 \\ x_2 \\ . \\ . \\ x_n \end{bmatrix} \quad (19)$$

We discuss the mean vector and covariance matrix

$$m_x = E\{x\} \quad (20)$$

$$C_x = E\{(x-m_x)(x-m_x)^T\} \quad (21)$$

The diagonal of C_x is the variance of vector. And we can find the correlation of any tow elements. Let A be a matrix whose rows are formed form the eigenvectors of C_x, ordered so that the last row is the eigenvector corresponding to the smallest eigenvalue.

Suppose that we use A as a transformation matrix to map the x into vectors denoted by y, as follows

$$y = A(x-m_x) \quad (22)$$

This expression is called the Hotelling transform. The covariance matrix of y is

$$C_y = AC_xA^T = \begin{bmatrix} \lambda_1 & & 0 \\ & \lambda_2 & \\ & . & \\ & . & \\ 0 & & \lambda_n \end{bmatrix} \quad (23)$$

The off-diagonal elements of this covariance matrix are 0, so the elements of the y vectors are uncorrelated.

The concept of aligning a 2-D object with its principal eigenvectors plays an important role in description. As noted earlier, description should be as independent as possible to variations in size, translation, and rotation. The ability to align the object with its principal axes provides a reliable means for removing the effects of rotation. The eigenvalues are the variances along the eigen axes, and can be used for size normalization. The effects of translation are account mind the fact that the method of description derived in this section is equally applicable to both regions and boundaries.

IV. Polynomial Approximation

After the text edit has been completed, the paper is ready for the template. Duplicate the template file by using the Save As command, and use the naming convention prescribed by your conference for the name of your paper. In this newly created file, highlight all of the contents and import your prepared text file. You are now ready to style your paper; use the scroll down window on the left of the MS Word Formatting toolbar.

A. *Lagrange Polynomial*

In this part, we introduce nth Lagrange Polynomial. This polynomial is given by

$$P(x) = f(x_0)L_{n,0}(x) + \cdots + f(x_n)L_{n,n}(x) = \sum_{k=0}^{n} f(x_k)L_{n,k}(x)$$

ISSN (ONLINE): 2454-9762
ISSN (PRINT): 2454-9762
Available online at www.ijarmate.com

International Journal of Advanced Research in Management, Architecture, Technology and Engineering (IJARMATE)
Vol. 2, Issue 3, March 2016

Where k=0, 1, 2,….,n

$$L_{n,k}(x)=\frac{(x-x_0)\cdots(x-x_{k-1})(x-x_{k+1})\cdots(x-x_n)}{(x_k-x_0)\cdots(x_k-x_{k-1})(x_k-x_{k+1})\cdots(x_k-x_n)}$$

B. *Error Term of Lagrange Polynomial*

Suppose $x_0, x_1, ..., x_n$ are distinct numbers in the interval [a, b] and $f \in C^{n+1}[a,b]$. Then, for each x in $[a,b]$, a number $\xi(x)$ (generally unknown) in (a,b) exists with

$$f(x)=P(x)+\frac{f^{(n+1)}(\xi(x))}{(n+1)!}(x-x_0)(x-x_1)\cdots(x-x_n)$$

Where $P(x)$ is the interpolating polynomial.

So the error is

$$e=|f(x)-P(x)|=\left|\frac{f^{(n+1)}(\xi(x))}{(n+1)!}(x-x_0)(x-x_1)\cdots(x-x_n)\right|$$

A practical difficulty with Lagrange interpolation is that since the error term is difficult to apply, the degree of the polynomial needed for the desired accuracy is generally not known until computations are determined. From this error term, we can approximate boundary which we want to descript.

V. Simulation And Results

All sequences were processed from frame decomposition, automatic ROI selection, globally despeckling, intracardiac mass segmentation, and nine feature extractions. The SRC was applied to the whole dataset to identify. The coarse-to-fine strategy helped to automatically select the ROI in an echocardiogram. The globally despeckling approach eliminated the noise while preserving important anatomical details. By means of the sparse representation, the initial mass contour was easily searched at a proper location.

The modified ACM guided the deformable contour in a desired manner, finally eliminating the ambiguity and converging to the true boundary.

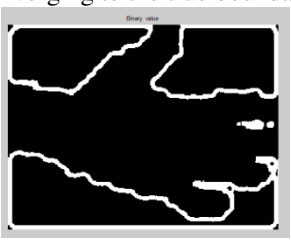

Binary image

b) Weiner filter

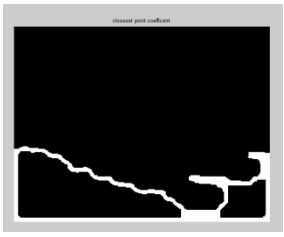

c) Closeset point co-efficient

d) Rough mask value

e) Final Image

VI. Conclusions

In this paper, a new method is proposed for the classification of intracardiac tumor and thrombi in the echocardiograms. The whole method is based on the sparse representation. The mass area in ROI is automatic defined by a coarse-to-fine strategy. A novel globally denoising approach combing the K-SVD and the NLM is employed to eliminate the speckle. The globally despeckling algorithm yields better noise attenuation and edge enhancement, without destroying the important cardiac structures. The K-SVD and a modified ACM with a new external force are applied to segment the mass. The better accuracy and simple implementation make the proposed method beneficial to help the cardiologists make a diagnosis before the surgery, providing a realistic performance benchmark for further research efforts.

References

[1] S. Warfield, K. Zou, and W. Wells, “Simultaneous truth and performance level estimation (STAPLE): An algorithm for the validation of image segmentation,” IEEE Trans. Med Imag., vol. 23, no. 7, pp. 903–921, Jul. 2004.

[2] M.-R. Nazem-Zadeh, E. Davoodi-Bojd, and H. Soltanian-Zadeh, “Atlasbased fiber bundle segmentation using principal diffusion directions and spherical harmonic coefficients,” NeuroImage, vol. 54, pp. S146–S164, 2011.

[3] K.H.Zou,S.K.Warfield,A.Bharatha,C.M.C.Tempany,M.R.Kaus, S. J. Haker,W.M.Wells, F. A. Jolesz, and R. Kikinis, “Statistical validation of image segmentation quality based on a spatial overlap index,” Acad. Radiol., vol. 11, no. 2, pp. 178–189, 2004.

[4] E. D. Angelini, O. Clatz, E. Mandonnet, E. Konukoglu, L. Capelle, and H. Duffau, “Glioma dynamics and computational models: A re- view of segmentation, registration, and in silico growth algorithms and their clinical applications,” Curr. Med. Imag. Rev., vol. 3, no. 4, pp. 262–276, 2007.

[5] M. Prastawa, E. Bullitt, S. Ho, and G. Gerig, “A brain tumor segmentation framework based on outlier detection,” Med. Image Anal., vol. 8, no. 3, pp. 275–283, 2004.

[6] J.Liu,J.K.Udupa,D.Odhner,D.Hackney,andG.Moonis,“Asystem for brain tumor volume estimation viaMR imaging and fuzzy connect-edness,” Comput. Med. Imag. Graph., vol. 29, pp. 21–34, 2005.

[7] T. Biswas et al., “Stereotactic radiosurgery for glioblastoma: Retro-spective analysis.,” Radiation Oncology, vol. 4, no. 11, p. 11, 2009.